Polarimetry: From the Sun to Stars and Stellar Environments
Proceedings IAU Symposium No. 305, 2015
A.C. Editor, B.D. Editor & C.E. Editor, eds.

DOI: 00.0000/X000000000000000X

SolpeX: the soft X-ray flare polarimeter–spectrometer for ISS

Janusz Sylwester[1], Stefan Płocieniak[1], Jarosław Bąkała[1], Żaneta Szaforz[1], Marek Stęślicki[1], Daniel Ścisłowski[1], Mirosław Kowaliński[1], Piotr Podgórski[1], Jose Hernandez[1] and Sergey Shestov[2]

[1]Space Research Centre, Polish Academy of Sciences,
51-622 Wrocław, ul. Kopernika 11, Poland
email: `js@cbk.pan.wroc.pl`

[2]P.N. Lebedev Physical Institute, Russian Academy of Sciences,
53 Leninskij Prospekt, 119991, Moscow, Russia
email: `sshestov@sci.lebedev.ru`

Abstract. We present an innovative soft X-ray spectro-polarimeter SolpeX. The instrument consists of three functionally independent blocks. They are to be included into the Russian instrument KORTES, to be mounted aboard the ISS. The three SolpeX units are: a simple pin-hole X-ray spectral imager, a polarimeter, and a fast-rotating drum multiple flat crystal Bragg spectrometer. Such a combination of measuring blocks will offer a new opportunity to reliably measure possible X-ray polarization and spectra of solar flares, in particular during the impulsive phase. Polarized Bremsstrahlung and line emission due to presence of directed particle beams will be detected and measurements made of the velocities of evaporated hot plasma. We discuss details of the construction of the SolpeX units. Delivery of KORTES with SolpeX to ISS is expected in 2017/2018.

Keywords. solar flares, soft X-rays, polarimetry, spectroscopy, ISS

---

1. Introduction

Studying the nature of flare X-ray sources is crucial for understanding the conversion of magnetic energy coming from reconnecting fields. A part of the non-potential magnetic energy is used to accelerate electrons and protons forming highly anisotropic beams propagating towards denser atmospheric regions along the field lines. These beams, while interacting with ambient dense plasma, release a small part of energy in the form of non-thermal Bremsstrahlung, expected to be polarized due to anisotropy of interactions. With SolpeX, we intend to detect this polarization for the first time in soft X-ray line and continuum emission at $\sim$3 keV, and additionally constrain the properties of electron beams by determining the orientation of magnetic field at the interaction region (Emslie *et al.* 2008). Models of interaction predict that the harder X-ray emission, consisting solely of continuum emission, should be highly polarized, with a polarization degree as high as 40% at 20 keV (Zharkova *et al.* 2010). The soft X-ray emission (at energies < 10 keV) containing emission lines seen atop the continuum is also expected to be polarized (Elwert & Haug 1970). The X-rays from anisotropic interactions are expected to dominate during the early impulsive phase of flares (durations seconds to minutes). The other processes contributing to polarization, although at a lower level, and the later flare phase are due to anisotropy of the electron distribution function within thermalized sources (Emslie & Brown 1980) and/or backscattering of the X-rays formed in the coronal X-ray source on lower-lying structures of solar atmosphere (Jeffrey & Kontar 2011).

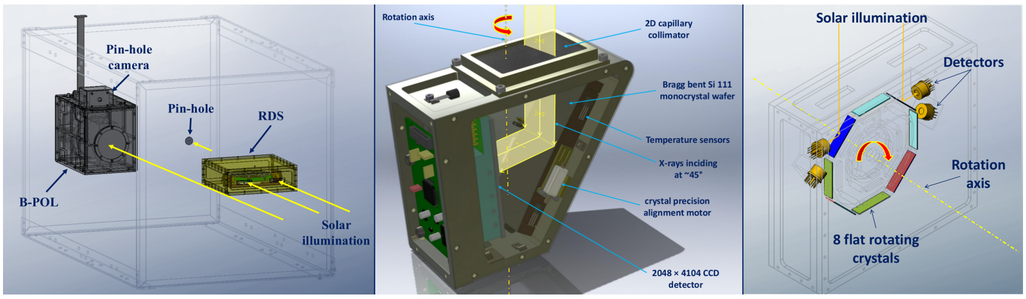

Figure 1. Left: Placement of pin-hole, B-POL and RDS blocks within Russian-build KORTES instrument; **Middle**: the polarimeter of B-POL; The rotation axis (1 rotation/second) is to be pointed towards the flare. The 2D collimator (2 arcmin × 2 arcmin) "isolates" the source from the rest of X-ray disk emission; **Right**: The RDS main components. Eight crystals (two of them identical) are fixed to the rotating (10 rps) drum. Bragg reflected spectra are recorded by four SDD detectors.

The importance of measuring polarization of X-ray flare emission was realized from the very beginning of the space era. The first attempts at detecting X-ray polarization from solar flares were made using polarimeters on-board Soviet Intercosmos satellites. The most recent determinations of solar flare X-ray polarization at the harder energy range were obtained from analysis of data collected by RHESSI and the SPR-N polarimeter on-board the CORONAS-F satellite.

Using RHESSI data McConnell *et al.* (2003) found a polarization of ∼18% in the energy range 20–40 keV. The source was an X-class solar flare of July 23, 2002 at 00:35 UT (SOL2002-07-23T00:35). For the same event and an additional X-class flare (SOL2003-10-28T11:06) the polarization at levels of 21%±9% and 11%±5% were reported by Boggs *et al.* (2006) at much higher energies (0.2–1 MeV). Suarez-Garcia *et al.* (2006) found for six X-class flares and one M-class flare values for the polarization degree in the range between 2% and 54% at an energy range between 100 to 350 keV.

Using the SPR-N polarimeter on-board the CORONAS-F satellite Zhitnik *et al.* (2006) found, among 90 analyzed flares, one event (X10 class flare SOL2003-10-29T20:37) which showed a significant polarization degree exceeding 70% at energies 40–100 keV and about 50% at lower energies (20–40 keV). For 25 events, the upper limits for the polarization were estimated to be between 8% and 40%.

All these determinations of X-ray polarization for flares were obtained using a Compton scattering technique. For polarized radiation, the azimuthal distribution of the scattered photons is no longer isotropic, but is related to the polarization vector of the incident photons. The energy resolution of the Compton polarimeters was rather coarse. Also, a low signal-to-noise ratio did not allow for high-time resolution determinations.

Therefore, we decided to try a different technique of polarization detection with the aim of studying the polarization in a softer X-ray band, i.e. the dependence of the total coefficient of Bragg reflection (close to the Brewster angle), on the orientation of the polarization vector relative to the crystal plane (cf. Fig. 1).

We describe below in some detail the construction of SolpeX blocks, designed to observe solar soft X-ray emission. The instrument consists of three measuring units placed within the KORTES instrument to be mounted by cosmonauts on top of the new Russian science module "*Nauka*" and to be delivered and attached to the ISS soon.

The SolpeX individual measuring units are:

- PHI — a simple **P**in-**H**ole soft X-ray **I**mager-spectrophotometer with moderate spatial (∼20 *arcsec*), spectral (0.5 keV) and high time resolution (0.1 *s*)

- B-POL the 3.9 Å – 4.6 Å (**B**ragg **POL**arimeter) with a low 1-2% linear polarization detection threshold.
- RDS — a fast **R**otating **D**rum X-ray **S**pectrometer with high time resolution (0.1 *s*)

In Fig. 1, we show the location of the units within the KORTES instrument. The RDS unit is placed close to the radiator, common for the entire instrument. The B-POL polarimeter is placed towards the rear of the instrument. This location is imposed by functionality, as the polarimeter's CCD detector is to be cooled down to below -20°C using the rotating radiator fixed to the rotating axis (acting also as the heat sink). On the side of the polarimeter, another smaller CCD is attached on which the X-ray image of the Sun from the pin-hole is projected. The pin-hole itself is mounted within the front-side of the instrument. KORTES is to be placed on the solar pointing platform attached to the ISS. This platform is directed towards the center of the solar disk. The illumination conditions at the location of KORTES are not ideal for making solar observations as the complicated mechanical structure of ISS causes substantial vignetting. Only $10-12$ *min* of uninterrupted illumination is available for every ISS orbit, so catching the impulsive phase of a flare will need some luck. Estimates indicate that in 2017, around the time of solar minimum, we can expect to observe the impulsive phases of ∼40 C-class flares, 5 M-class flares and 0.5 X-class flare during one year of instrument operation in orbit. The KORTES instrument will be delivered to ISS by a cargo ship and then fixed to the *Nauka* module by cosmonauts. After the mission is completed (or in case of failure), the instrument will return to the ground for post-flight checks. The data from the instrument will be transmitted on-line to the recorder inside ISS, so practically unlimited storage is available on hard disk. A selected part of the information will be telemetered down on-line for prompt analysis leading to software corrections and upgrades. The instrument can be operated round the clock, also during the night-portions of the orbit for the calibration purposes or measurements of non-solar astrophysical sources. We describe below each block of SolpeX in more detail.

2. Pin-Hole soft X-ray Imager-spectrophotometer — PHI

In order to increase the signal-to-noise ratio, the polarimeter unit will be equipped with a 2D collimator which will limit the field of view to ∼2 *arcmin*, centered on the flare. Therefore, a reliable pointing system is required as well as a system to localize the source within the frame of KORTES instrument coordinate system. A simple pin-hole camera

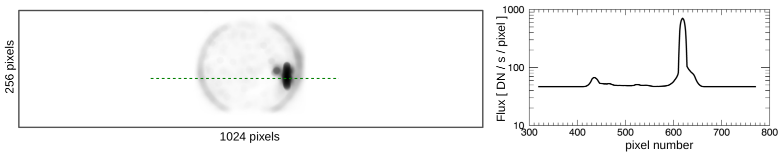

Figure 2. Simulated image of X-ray Sun with C5 class flare in progress projected on the pinhole camera CCD (left). The signal profile "observed" along the dashed line cut is shown to the right.

will be sufficient for this purpose. In order to achieve adequate X-ray photon statistics, the pin hole will have $\sim 1\,mm^2$ size, a focal length of 60 *cm* and will be equipped with a 256×1024 pixels detector of $26\,\mu m$ pixel size (e2v CCD30-11 Back Illuminated). Such a configuration will project the X-ray solar image of $\sim 5.5\,mm$ diameter which corresponds to ∼215 detector pixels. The simulated solar C5.0-class flare image to be seen by this camera is shown in Fig. 2. A large part of the CCD signal from sections away from solar disk will be used to determine orbital particle flux at the ISS current location along the

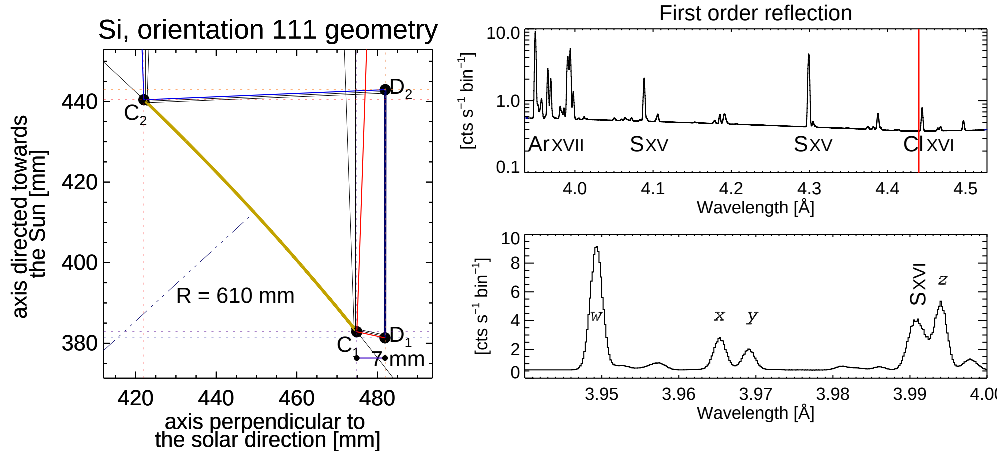

Figure 3. Left: Cylindrical mono-crystal wafer of Si with 610.0 *mm* radius of curvature geometry. Points C_1 and C_2 define "active" edges of the Si crystal and D_1 and D_2 respective edges of the CCD detector. The yellow–green line represents the curved surface of the monocrystal wafer cut along the 111 plane. Blue and red lines shows the photon paths for the sources located at the boundary of 2D collimator FOV (angles are exaggerated for clarity). **Right:** Simulated spectrum of an M5 flare to be recorded over the entire spectral range (upper-part). The position of the wavelength corresponding to the Brewster angle is indicated with red vertical line. Enlarged portion of the spectrum covering the principal Ar XVII triplet lines is shown below.

orbit with high time resolution. This signal will also be used to estimate the background for the large polarimeter CCD (see below).

From the images similar to that shown in Fig. 2 (to be collected every 0.1 *s*) the soft X-ray light curves of individual active regions will be analyzed in real-time by the on-board software in order to detect and locate flares. A 2D Gaussian elliptical profile will be fitted to individual stronger brightenings and their central position will be determined. This position will be passed to the B-POL pointing system in order to lock the position of the polarimeter rotation axis on this target. The limb-brightened rim will be used to determine the position of the solar disk edge. For low intensity areas, where single counts (per CCD dump) are observed in respective pixels, the spectra will be determined with moderate spectral resolution (~200 eV).

3. X-ray polarimetry of solar flares — B-POL

The heart of B-POL polarimeter (cf. Fig. 1) consists of cylindrically bent mono-crystal and a large detector (e2v back illuminated CCD261-84, 2048 × 4096; 30.7 *mm* × 61.6 *mm*) fixed together at the angle of ~45°. This unit will be continuously rotating along the axis directed to the source selected from the pin-hole image. The rotation rate has been selected to be $1\,s^{-1}$ which is a compromise between the CCD read-out time and expected rate of polarization variations (seconds). The pointing of the rotation axis will usually be moved towards the brightest region of interest (i.e. the flare) by turning the support of crystal-detector section within the angular range of ±2°. We elected to use Silicon 111 crystal surface bent cylindrically to a 610.00 *mm* radius as the dispersive medium. The adopted crystal-detector geometry set-up allows spectra to be obtained in the spectral range 3.9 Å − 4.5 Å with exceptionally good spectral resolution ~0.00014 Å/bin. This is better than the instrumental spectral resolution (0.00034 Å) and is much smaller than the thermal/turbulent width of emission lines. Details of the crystal-detector placement and example of the spectrum to be measured for the M5.0 flare are given in Fig. 3

Table 1. *Crystals selected for the RDS.*

No	Crystal	Orientation	2d [Å]	Wavelenght range 1 [Å]	Wavelenght range 2 [Å]
1.	Si	400	2.715	1.397 – 2.331	0.270 – 1.796
2.	Si	220	3.840	1.977 – 3.298	0.391 – 2.541
3.	2×Si*	111	6.271	3.228 – 5.385	0.639 – 4.150
4.	Quartz	$10\bar{1}1$	6.684	3.441 – 5.740	0.681 – 4.423
5.	Quartz	$10\bar{1}0$	8.514	4.383 – 7.312	0.868 – 5.635
6.	ADP	101	10.648	5.482 – 9.145	1.086 – 7.047
7.	KAP	001	26.640	13.72 – 22.88	12.72 – 17.63

As shown in Fig. 3, in the selected spectral range a number of strong emission lines are present, due to Ar XVII, Si XV, Si XVI as well as the much weaker Cl XVI triplet lines. The observed spectral range will be recorded for Bragg incidence angles close to the Brewster angle, and so their reflected intensities will depend on the degree of linear polarization and respective orientation of the polarization vector relative to crystal surface.

During the rotation of the crystal-detector unit, the position of the crystal dispersion plane with respect to incoming light beam will continuously change. This will give rise to a modulation of the reflected beam intensity provided the incident X-ray beam is linearly polarized. It has been shown with the Electron Beam Ion Trap (EBIT: Beiersdorfer *et al.* 1996) that the polarization of the He-like triplet lines for iron and lighter elements can be substantial and depends on the relative orientation of the EBIT particle beam and the crystal polarimeter plane. From Fig. 1 of this Paper it follows that, for Ar XVII (as well as for much weaker Cl XVI triplet lines), the degree of polarization of w and x lines can be close to 0.6 and -0.6 respectively. This level of polarization would easily be detected by B-POL for stronger flares.

The Ar as well as S lines are nearly always present in solar X-ray spectra for activity above GOES B5.0 class level (Sylwester *et al.* 2010). Therefore, the B-POL will record spectra of flares and stronger active regions for most of the time. This will also allow for studies of thermal plasma properties like turbulence, directed motions, differential emission measure distribution and elemental composition. However, lines of only few elements are present in the B-POL spectral range suitable for polarization detections. In order to extend the spectral coverage over the entire soft X-ray range from 1 Å to 23 Å, we included within KORTES a novel RDS spectrometer described below.

4. The fast-rotating X-ray spectrometer — RDS

The fast-**R**otating **D**rum X-ray **S**pectrometer will allow us to investigate very fast changes of solar spectra including lines and continuum. Precise line Doppler shift measurements will be possible. The novelty of the approach is that in order to assign the wavelength to each photon, Bragg-reflected from the crystal, we will use the timing information on the photon arrival on the SDD detector. Using such modern detectors (Ketek, Vitus–H80), the arrival time can be determined with an accuracy of ∼1 *microsecond*. In one microsecond, the drum with the crystals will rotate by ∼10 *arcsec* only, so the line wavelength smear corresponding to such a small change of the incidence angle can be neglected and the actual photon wavelength can be derived with precision better than the width of the instrumental function (i.e. crystal rocking curve). As seen in Fig. 1 (right panel), the flat crystals are attached to an octagonal drum rotating at high rate (10 rps). The drum geometry is selected such that the solar X-rays illuminate a pair of the rotating crystals, from which the Bragg-reflected photons are being recorded by two pairs of SDD detectors. Each detector records spectra at slightly different Bragg angle. We will use detectors characterized by a very fast response (∼1 μs). By measuring the photon arrival times on every detector, the respective crystal incidence angles can easily be determined and converted to corresponding incoming photon wavelengths (or equivalently energies) provided the calibration of the system on the ground is carefully done. A histogram of spectra will be built as time progresses, with the time resolution depending on the source intensity. For flares above M5.0 class, enough photons will be recorded to study spectra variability on a time scale of ~ 1 second.

The symmetrical location of detectors on both sides of the drum (with respect to the direction towards the Sun) represents the configuration necessary to fulfil the tasks of a "dopplerometer" (Sylwester *et al.* 2015). We plan to use eight flat crystals, two of them identical (see Table 1 for details). For every crystal two spectral wavebands are given. The first band is covered by the "front" pair of detectors (those closer to the Sun). The second waveband is covered by the rear pair. Two identical crystals marked with a star are placed in the classical dopplerometer configuration. With all the rotating crystals a wide continuous spectral range extending from 0.3 Å to 22.8 Å will be covered every 0.1 s. This will allow us to determine spectral line fluxes and and doppler shifts for all abundant elements from oxygen to iron emitted by a hot flaring plasma between 1 MK and 50 MK. These data will support the measurements of spectra made using the B-POL unit.

5. Summary

The SolpeX spectrometer consisting of three blocks will be placed on the ISS as a part of KORTES Russian instrument. SolpeX consists of the B-POL Bragg polarimeter, RDS rotating spectrometer with eight flat crystals and a simple pin-hole imager. With these three units, the following measurements will be performed in the soft X-ray range for flares and/or active regions (AR) of temperature 1 MK and above.

- individual AR/flare light curves and their coordinates with time resolution 0.1 *s*,
- flare linear polarization vector characteristics at energy $\sim$3 keV every $1-10$ *s*,
- AR/flare spectra in the entire soft X-ray range, with time resolution 0.1 *s*.

These measurements will complement each other allowing substantial progress in understanding the processes of magnetic energy release, transport and dissipation in various solar coronal structures, flares in particular. The success of this project will pave the way for building a larger instrument, based on a similar principles, to be placed on a larger future solar satellite .

Acknowledgements: We would like to thank Professor Ken J.H. Phillips for corrections and helpful comments. We acknowledge financial support from the Polish *National Science Centre* grant 2013/11/B/ST9/00234.

References

P. Beiersdorfer, P., Vogel, D. A., Reed, K. J. *et al.* 1996, *Physical Review A*, 53, 3974
Boggs, S. E., Coburn, W. & Kalemci, E. 2006, *ApJ*, 638, 1129
Elwert, G. & Haug, E. 1970, *Solar Physics*, 15, 234
Emslie, A. G. & Brown, J. C. 1980, *ApJ*, 237, 1015
Emslie, A. G., Bradsher, H. L. & McConnell, M. L. 2008, *ApJ*, 674, 570
Jeffrey, N. L. S. & Kontar, E. P. 2011, *A&A*, 536, 93
McConnell, M. L., Smith, D. M., Emslie, G. *et al.* 2003, *Proc. SPIE*, 4843, 1382
Suarez-Garcia, E., Hajdas, W., Wigger, C. *et al.* 2006, *Solar Physics*, 239, 149
Sylwester, B., Sylwester, J. & Phillips, K. 2010, *A&A*, 514, A82
Sylwester, J., Kordylewski, Z., Płocieniak, S. *et al.* 2015, *Solar Physics*, 290, 2
Zharkova, V. V., Kuznetsov, A. A. & Siversky, T. V. 2010, *A&A*, 512, 8
Zhitnik, I. A., Logachev, Yu. I., Bogomolov, A. V. *et al.* 2006, *Solar System Research*, 40, 93